

Influence of relaxation on the size distribution of monatomic Ag chains on the steps of a vicinal Pt surface

V. I. Tokar^{1,2} and H. Dreysse¹¹IPCMS-GEMM, UMR 7504 CNRS, 23 rue du Loess, F-67034 Strasbourg Cedex, France²Institute of Magnetism, National Academy of Sciences, 36-b Vernadsky strasse, 03142 Kiev-142, Ukraine

(Received 1 September 2006; revised manuscript received 10 May 2007; published 2 August 2007)

Recently, Gambardella *et al.* [Phys. Rev. B **73**, 245425 (2006)] determined experimentally the size distribution of the chains of Ag atoms self-assembled on the steps of a vicinal Pt surface. The experimental results were interpreted by the authors within a simple model which predicted the monotonous distribution of the chain sizes. The data, however, exhibit a nonmonotonous behavior with a maximum. We show that if additional interactions unaccounted for in the model introduce a sufficiently large positive curvature of the chain energy, the size distribution can be fitted to the experimental data with high accuracy. We discuss several interactions which may provide the necessary curvature.

DOI: 10.1103/PhysRevB.76.073402

PACS number(s): 81.15.Aa, 68.55.Ac

One dimensional (1D) monatomic chains may find important nanotechnological applications, e.g., as nanowires in microelectronic devices,¹ so it is important to develop techniques of their controlled growth. The self-assembly of such chains of varying lengths has been observed in some heteroepitaxial systems.^{1–14} From the point of view of applications, it would be desirable that the chains were of similar length and regularly spaced. Therefore, the understanding of the mechanisms which define the chain sizes and interchain spacings would be of considerable interest.

In the present Brief Report, we will discuss the recent study of Gambardella *et al.*¹³ (hereafter referred to as I) of the growth of monatomic chains of Ag atoms on the steps of the vicinal Pt(997) surface. The distribution of Ag chain lengths, as well as of interchain separations, was established experimentally and then compared with an atomistic 1D model with pairwise interatomic interactions restricted to nearest neighbor atoms [see Fig. 1(a)]. According to the authors, a satisfactory agreement was found only for the chains longer than five atoms. The statistics for shorter chains were not reproduced. It was suggested that the disagreement between theory and experiment in the small island limit may be due to the presence of the epitaxial strain that was not accounted for in the model.

The theory developed in I may be summarized as follows. The probability of length distributions of the atomic chains and the interchain gaps is described by the geometric distribution which, presumably, is the simplest one because it is the only discrete memoryless distribution.^{15,16} In the case of atomic chains, it means that the probability of attachment of an atom to the chain (let us denote it by q) does not depend on the chain length l . We note that this length independence implicitly presumes that interatomic interaction is restricted to nearest neighbor atoms at most

$$P_l = (1 - q)q^{l-1}. \quad (1)$$

The distribution is fully characterized by the parameter q which, in the case under consideration, can be fixed by fitting the average chain length

$$\langle l \rangle = \sum_l l P_l = 1/(1 - q) \quad (2)$$

to the value M/K , where M is the total number of adsorbed atoms (hence, the sum of all chain lengths) and K the total number of chains. Experimentally, these numbers in I were found to be equal to 1811 and 211, respectively. In this way Eq. (12) of I can be reproduced. Equation (13) of I is obtained similarly by replacing M with $N - M$, the total number of free deposition sites ($N = 5816$ is the total number of deposition sites). Due to the 1D topology, the number of islands K is equal to the number of gaps (up to at most ± 1 , which is not essential for large values of K).

From Fig. 2(b) of I, it can be seen that while the experi-

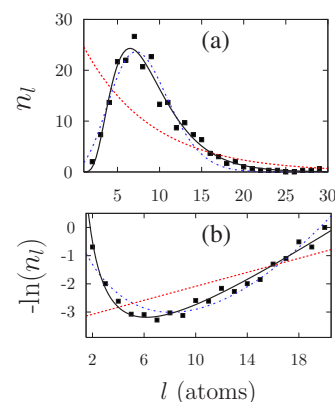


FIG. 1. (Color online) (a) The black squares are the number of Ag chains of length l self-assembled on the steps of the vicinal Pt(997) substrate at temperature $T=400$ K and coverage $\theta=0.3$ as established experimentally in Ref. 13; the dashed curve is theoretical fit according to Eq. (12) from the same reference. The dash-dotted line is the fit corresponding to the Coulomb repulsion and the solid curve to the dipole-dipole interaction. (b) Same as above on the logarithmic scale for the interval of chain lengths where the cluster numbers n_l are nonzero. According to Eq. (3), the curvature of the data is completely due to the nonlinearity of $E(l)$.

mental data on the gap sizes are in reasonable agreement with the geometric distribution, the agreement with the data on atomic chains is rather poor, as can be seen from Fig. 1 of the present Brief Report. Most noticeable is the qualitative distinction between the monotonous theoretical curve and the monomodal experimental distribution with a pronounced maximum around $l=7$.

To understand the origin of this discrepancy, we invoke the general approach of Ref. 17 which allows us to express the chain length distribution via their energies $E(l)$ as

$$n_l = C \exp\left[\frac{\mu l - E(l)}{k_B T}\right], \quad (3)$$

where n_l is the number of chains of length l ; μ and C are some parameters. In Ref. 17, this form of the size distribution was derived on the basis of the mass action law for two dimensional (2D) islands with l being the total number of atoms in the island. The applicability to 1D islands may be justified by the observation that monatomic chains formally are 2D islands with the widths equal to 1. This observation was confirmed with the use of the Monte Carlo simulations in Ref. 18. Furthermore, the exact solution for a class of 1D models of strained epitaxy obtained in Refs. 19 and 20 also gives the cluster size distribution of the type of Eq. (3). Finally, the distribution derived in I can also be cast in the form of Eq. (3) with the chain energy linear in the chain length,

$$E(l) = V_{NN}(l-1), \quad (4)$$

where V_{NN} is the energy of coupling of nearest neighbor atoms. [The intrachain energy term in Eq. (4), $2KE_b$ in I, can be transformed into Eq. (4) with the use of techniques presented in Refs. 19–21.] Here, we would like to note that the l -independent term V_{NN} in Eq. (4) can be unified with C in Eq. (3) in a single normalization constant. Similarly, μl and $V_{NN}l$ can be unified into a term linear in l . Thus, the dashed line in Fig. 1 is a two parameter fit to the experimental data. In I, the parameters were fixed so as to reproduce the experimental values of the total numbers of adatoms M and of the islands K .

In order for n_l in Eq. (3) to exhibit the maximum seen in experimental data, the usual conditions for the derivatives should be fulfilled at some value of length $l=l_m$,

$$\begin{aligned} \mu - E'(l)|_{l=l_m} &= 0, \\ E''(l)|_{l=l_m} &> 0, \end{aligned} \quad (5)$$

where, for the discrete derivatives denoted by primes, we assumed the conventional rules of differentiation to be approximately valid. Equation (5) means that the chain energy should be a convex function of l in the vicinity of l_m . This, in particular, precludes the linear dependence of the energy on the chain length [Eq. (4)] which was explicitly assumed in I. Thus, in order to be consistent with experimental data, the chain energy should contain nonlinear terms which would provide the necessary positive curvature in Eq. (5). Below, we consider some plausible causes of such nonlinearity.

It is widely believed that the elastic strain due to the lattice size misfit between the substrate and the growing over-

layer plays a major role in heteroepitaxial deposition. Such a misfit is present in the majority of heteroepitaxial systems because of the dissimilarity of sizes of different atoms. In theoretical studies, it is conventional to account for the elastic interactions on the surface by introducing the dipole-dipole interatomic repulsion described by the potential^{22,23}

$$V_D(r) = \frac{q}{r^3}, \quad (6)$$

where $q>0$ is the interaction strength and r the interatomic distance measured in surface lattice units.

Furthermore, there always exists some charge transfer between the adatoms and the substrate bulk due to the rapid variation of the electrostatic potential near the surface. According to Ref. 24, the charge transfer in the system under consideration is so strong (about $0.43e/\text{Ag}$ atom) that it enhances the surface stress inside the Ag layer more than an order of magnitude in comparison with the elasticity theory. This correlates with the weakening of the chemical attraction, $|V_{NN}|=2E_b \approx 0.166$ eV, as obtained from the experimental data in I (in Sec. III) in comparison with the theoretical estimate, $|V_{NN}|=0.57$, obtained in Ref. 19 (see Sec. III E) in which the charge transfer was not taken into account. Qualitatively, the contribution of the charge transfer into the curvature of the chain energy at short distances can be modeled within the point charge approximation with the unscreened Coulomb potential

$$V_C(r) = \frac{Q^2}{r}, \quad (7)$$

where Q^2 is the charge transfer per atom.

As can be seen from Eq. (A1) in the Appendix, the contribution of Eqs. (6) and (7) into the chain energy have a complicated structure with the number of terms in the double sums growing as $\sim l^2$. To simplify the consideration, in Eq. (A2), we show that the second discrete derivative of each of these contributions is equal to the potential V_D or V_C itself. Thus, in order to have the positive curvature of the chain energy, the nonlinear contribution into the chain energy should be dominated by repulsive interactions. Now, approximating the discrete derivatives with the continuous ones and integrating Eq. (A2), we arrive at

$$\begin{aligned} W_D(l) &\approx \frac{q}{2l} + C_1 l + C_2, \\ W_C(l) &\approx Q^2 l \ln l + C_1 l + C_2, \end{aligned} \quad (8)$$

where C_1 and C_2 are the integration constants. As previously, the linear term may be unified with the term μl while the constant can be incorporated into the normalization factor, so now, Eq. (3) contains three parameters (two parameters as previously plus q or Q^2) to fit the experimental data. The chain energy can be written as

$$E(l) = \tilde{V}_{NN}(l-1) + \tilde{W}(l) + \text{const}, \quad (9)$$

where \tilde{V}_{NN} is the parameter V_{NN} corrected on the linear in l contributions from $W_{D,C}$ while $\tilde{W}(l)$ is a relaxationlike term

where l tends to zero at large length because the constant and the linear terms are included in other terms entering Eq. (9). [Though the Coulomb contribution in Eq. (8) does not have such asymptotics, we consider Eq. (8) to be valid only at small values of l while at large length, the relaxation behavior will take place because in metallic systems, the Coulomb interaction is always screened at large distances.]

The results of the fit of Eq. (9) to the experimental data are shown in Fig. 1 by the dashed-dotted line for the Coulomb case and by the solid line for the dipole interaction. As we can see, the agreement with the experimental data is good in both cases and is almost perfect in the dipole case.

The good agreement achieved, however, is based essentially only on the positive curvature of the relaxation energy which may have other origins than the forces discussed above. Moreover, in a more accurate theory, we would need some interactions which provide the positive curvature of the island energy as above but at the same time will be negligible beyond nearest neighbor interactions. Such short range forces are necessary in order to not distort the gap distribution, which, in the first approximation, we (following I) consider to be described by the geometric distribution corresponding to negligible interisland interaction. Besides the Ag/Pt system under consideration, the necessity for the repulsive short range forces to explain experimental data on the N/Cu(100) system was also noted in Ref. 25.

The forces of this type were established theoretically in Ref. 19 as a consequence of the misfit. It was shown that even if the substrate is rigid and the mechanism of interatomic interactions envisaged in Refs. 22 and 23 is not operative, the size mismatch with the substrate leads to the direct influence of neighbor atoms on each other, thus introducing their effective repulsion. Long range repulsion, however, is absent because the misfit is usually small (typically a few percent), so the atoms separated by even one empty site practically do not interact. The possibility to fit the data of I within the model based on this type of elastic relaxation can be seen from Fig. 4 of Ref. 19. We did not show the corresponding curve on Fig. 4 because it would largely overlap with the curve corresponding to the dipole interaction by providing an even better fit to the data. The latter is mainly because the relaxation term W_l in the theory of Ref. 19 contains an additional fitting parameter.

Finally, it is important to point out that in metallic systems, all interactions cannot be reduced to pairwise forces, but they may contribute to the convexity of the chain energy. For example, the convex behavior is typical for the energy of metallic clusters.^{26,27} The cause is the physics of electron collectivization and the formation of energy bands. Qualitatively, this can be illustrated by the simple free-electron model of the one dimensional band structure in the gold chains on the NiAl(110) surface proposed in Ref. 8. In a 1D potential well with infinitely high walls, the kinetic energy of an electron is defined by the square of the quasimomentum,

$$k^2 = (\pi n/L)^2, \quad (10)$$

where n is the quantum number and L the length of the box which is roughly equal to the chain length: $L \approx l$. From

Eq. (10), it can be seen that both the energies of individual electrons and the total chain energy obtained as the sum over n over the filled states are the convex functions of l . We will not proceed further with the model calculation of the chain energy but only note that its curvature due to the band formation effects is quite large, as can be seen from the experimental behavior of the bottom of the electron band in Au chains shown in Fig. 4(C) of Ref. 8.

In conclusion, we would like to stress that disordered heteroepitaxial surface structures are generally complex systems lacking many symmetries which simplify the study within *ab initio* approaches. In our opinion, one dimensional structures on vicinal surfaces present convenient model systems for theoretical studies. This is because, firstly, in the *ab initio* calculations of various cluster energies needed in statistical simulations,¹¹ the restriction to only 1D clusters (or chains) presents a very significant reduction in computational effort and, secondly, the simplicity of 1D statistics (as, e. g., the absence of phase transitions) allows for an accurate calculation of statistical quantities, such as the cluster size distributions.²⁰

To sum up, in this Brief Report, we have shown that if the length distribution of 1D atomic chains in thermodynamic equilibrium has a maximum, then the length dependence of the chain energy exhibits a positive curvature. The latter may be caused by the repulsive forces, such as the substrate-propagated long range dipole-dipole^{22,23} and the Coulomb interactions or the short range forces like those introduced in Ref. 19. Additional contribution may originate from the collectivization of electrons due to the band formation inside the chains, as observed experimentally in Refs. 8 and 9. In general, any intrachain phenomenon leading to the relaxationlike behavior of the chain energy with positive curvature may contribute to the observed cluster size distribution. The relative importance of these contributions is difficult to assess within the phenomenological approach used by us. We hope that the simplicity of the quasi-one-dimensional geometry of the Ag/Pt(997) system will make the *ab initio* determination of the parameters necessary for the quantitative modeling of this and similar systems feasible.

The authors acknowledge CNRS for support of their collaboration. The authors are grateful to P. Gambardella for providing them with the experimental data prior to their publication. One of the authors (V.I.T.) expresses his gratitude to the University Louis Pasteur de Strasbourg and IPCMS for the hospitality.

APPENDIX

Let us consider the chain of atoms of length $l+1$ with the first atom placed on site 0 and the last one on site l . We unify the cases of the dipole and the Coulomb interactions [Eqs. (6) and (7)] by considering the general potential $V(r)$. The contribution to the total chain energy associated with the interaction between all atoms inside the chain is

$$\begin{aligned}
W(l+1) &= \frac{1}{2} \left(\sum_{l'=1}^l \sum_{l''=0}^{l'-1} + \sum_{l''=0}^{l-1} \sum_{l'=l''+1}^l \right) V(|l_i - l'|) \\
&= \frac{1}{2} \left(\sum_{l'=1}^{l-1} \sum_{l''=0}^{l'-1} + \sum_{l''=0}^{l-2} \sum_{l'=l''+1}^{l-1} \right) V(|l_i - l'|) \\
&\quad + \sum_{l''=0}^{l-1} V(l - l''), \tag{A1}
\end{aligned}$$

where, on the first line, we sum the interaction of the atom i with the atom l' on the left and on the right of i and, on the second line, we gathered the terms which would correspond to $W(l)$. Thus, the discrete derivatives are

$$\begin{aligned}
W'(l+1) &\equiv W(l+1) - W(l) = \sum_{l''=0}^{l-1} V(l - l''), \\
W''(l+1) &\equiv W'(l+1) - W'(l) = V(l). \tag{A2}
\end{aligned}$$

-
- ¹J. H. G. Owen, K. Miki, and D. R. Bowler, *J. Mater. Sci.* **41**, 4568 (2006).
²Y. W. Mo and F. J. Himpsel, *Phys. Rev. B* **50**, 7868 (1994).
³P. Gambardella, M. Blanc, H. Brune, K. Kuhnke, and K. Kern, *Phys. Rev. B* **61**, 2254 (2000).
⁴A. Dallmeyer, C. Carbone, W. Eberhardt, C. Pampuch, O. Rader, W. Gudat, P. Gambardella, and K. Kern, *Phys. Rev. B* **61**, R5133 (2000).
⁵F. Picaud, C. Ramseyer, C. Girardet, and P. Jensen, *Phys. Rev. B* **61**, 16154 (2000).
⁶P. Segovia, D. Purdie, M. Hensenberger, and Y. Baer, *Nature (London)* **402**, 504 (1999).
⁷P. Gambardella, A. Dallmeyer, K. Maiti, M. C. Malagoll, W. Eberhardt, K. Kern, and C. Carbone, *Nature (London)* **416**, 301 (2002).
⁸N. Nilius, T. M. Wallis, and W. Ho, *Science* **297**, 1853 (2002).
⁹J. N. Crain and D. T. Pierce, *Science* **307**, 703 (2005).
¹⁰S. J. Koh and G. Ehrlich, *Phys. Rev. B* **62**, R10645 (2000).
¹¹S. J. Koh and G. Ehrlich, *Phys. Rev. B* **60**, 5981 (1999).
¹²M. A. Albao, M. M. R. Evans, J. Nogami, D. Zorn, M. S. Gordon, and J. W. Evans, *Phys. Rev. B* **72**, 035426 (2005).
¹³P. Gambardella, H. Brune, K. Kern, and V. I. Marchenko, *Phys. Rev. B* **73**, 245425 (2006).
¹⁴J. N. Crain, M. D. Stiles, J. A. Stroscio, and D. T. Pierce, *Phys. Rev. Lett.* **96**, 156801 (2006).
¹⁵E. W. Weisstein, from MathWorld, Wolfram web resource (<http://mathworld.wolfram.com/Memoryless.html>).
¹⁶E. W. Weisstein, from MathWorld, Wolfram web resource (<http://mathworld.wolfram.com/GeometricDistribution.html>).
¹⁷C. Priester and M. Lannoo, *Phys. Rev. Lett.* **75**, 93 (1995).
¹⁸V. I. Tokar and H. Dreyssé, *Phys. Rev. B* **74**, 115414 (2006).
¹⁹V. I. Tokar and H. Dreyssé, *Phys. Rev. B* **68**, 195419 (2003).
²⁰V. I. Tokar and H. Dreyssé, *Phys. Rev. E* **68**, 011601 (2003).
²¹J. Vavro, *Phys. Rev. E* **63**, 057104 (2001).
²²K. H. Lau and W. Kohn, *Surf. Sci.* **65**, 607 (1977).
²³V. I. Marchenko and A. Y. Parshin, *Sov. Phys. JETP* **52**, 129 (1980).
²⁴A. Grossmann, W. Erley, J. B. Hannon, and H. Ibach, *Phys. Rev. Lett.* **77**, 127 (1996).
²⁵H. Ellmer, V. Repain, S. Rousset, B. Croset, M. Sotto, and P. Zeppenfeld, *Surf. Sci.* **476**, 95 (2001).
²⁶P. Villaseñor-González, J. Dorantes-Dávila, H. Dreyssé, and G. M. Pastor, *Phys. Rev. B* **55**, 15084 (1997).
²⁷O. Diéguez, M. M. G. Alemany, C. Rey, P. Ordejón, and L. J. Gallego, *Phys. Rev. B* **63**, 205407 (2001).